Applied Physics A (2022) 128:167
https://doi.org/10.1007/s00339-022-05307-4

Applied Physics A
Materials Science & Processing

Kinetic, isotherm, and thermodynamic studies on Cr(VI) adsorption using cellulose acetate/graphene oxide composite nanofibers

Indah Raya[1] · Gunawan Widjaja[2] · Zaid Hameed Mahmood[3] · Abed J. Kadhim[4] · Kabanov Oleg Vladimirovich[5,6] · Yasser Fakri Mustafa[7] · Mustafa M. Kadhim[8,9] · Trias Mahmudiono[10] · Ismail Husein[11] · Leila Kafi-Ahmadi[12]

Received: 11 October 2021 / Accepted: 10 January 2022 / Published online: 1 February 2022

Abstract

In the present study, cellulose acetate/graphene oxide (CA/GO) composite nanofibers were prepared via the electrospinning method to remove Cr(VI) ions from aqueous solution via adsorption process in a batch mode. The impact of adsorption parameters, including contact time, pH, Cr(VI) concentration, and temperature was investigated to obtain the optimum conditions for the uptake of maximum Cr(VI) ions from water within a short time. The kinetic data of Cr(VI) adsorption were well fitted by pseudo-first-order and pseudo-second-order kinetic models, whereas Redlich-Peterson, Langmuir and Freundlich, isotherm models were used to describe the equilibrium data of Cr(VI) adsorption by the CA/GO nanofibers. The effect of temperature on the adsorption capacity of Cr(VI) ions using the nanofibers indicated that the higher temperatures were favorable for higher adsorption of Cr(VI) ions using the nanofibers. The thermodynamic parameters results indicated the spontaneous and endothermic of Cr(VI) sorption nature using the CA/GO nanofibrous adsorbent. The maximum monolayer adsorption capacity of nanofibers toward Cr(VI) ions sorption was 422.3 mgg^{-1} which was comparable with other adsorbents. The reusability of composite nanofibers was carried out for five adsorption–desorption cycles. The obtained results exhibited the high capability of CA/GO nanofibrous adsorbents for Cr(VI) ions sorption from actual wastewater.

Graphical abstract

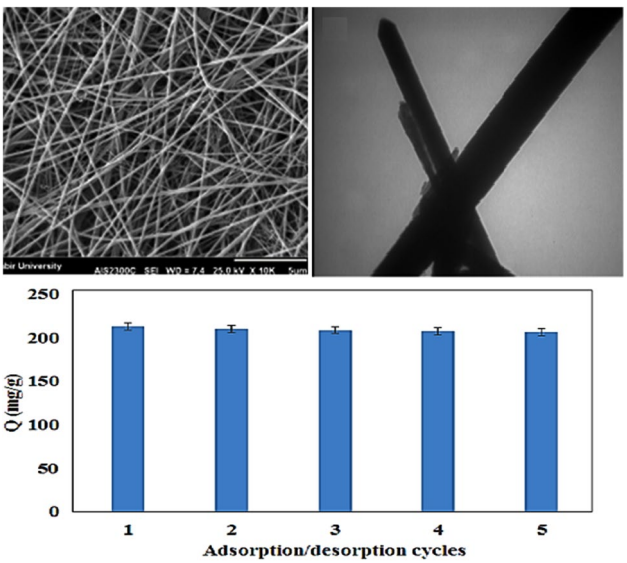

Keywords Nanofibers · Cellulose acetate · Cr(VI) · Graphene oxide · Adsorption

Extended author information available on the last page of the article

1 Introduction

The discharge of chromium compounds from wastewater of different industries such as pigments, glass, metal finishing, electroplating, electrical equipment, and magnetic tapes into the environment produces high toxicity and endanger animal, plant, and human life [1–7]. The permissible concentration of Cr(VI) for drinking water should be lower than 50 μgmL^{-1} based on World Health Organization [2]. The high level of Cr(VI) ions in water is mutagenic and carcinogenic for various organs [2]. Therefore, the Cr(VI) ions in water event its lower level should be removed before its discharge to the environment. Various techniques including precipitation [8–13], adsorption [14–17], advance oxidation [18–20], membrane filtration [21], coagulation [22] and so on were used to remove Cr(VI) ions and other contaminants from water. The adsorption process is a favorable method for decreasing the level of Cr(VI) ions in water due to its low cost and good efficiency [23]. The efficiency of adsorption process is related to the level of available active sites of adsorbent for conjugating with adsorbate ions and their adsorption. Nanofibers prepared by the electrospinning method are good candidates for the adsorption of various contaminants from water due to their high porosity and large specific surface area [24–31]. Cellulose-based nanofibers could be considered as effective adsorbents for the removal of toxic matters from water [32, 33]. However, using pure cellulose is limited due to the easier dissolving in water. Cellulose acetate (CA) as ester cellulose exhibited higher mechanical properties in water than pure cellulose. Recently, the electrospun CA nanofibers prepared by the electrospinning method are recommended for different wastewater treatments [34–36]. Furthermore, inorganic nanomaterials such as carbon nanotubes [26], titanium dioxide [37], ferrite nanoparticles [38] were incorporated into the CA nanofibers to increase the strength and adsorption capacity of CA nanofibers. For instance, single-walled carbon nanotubes, ferrite, and titanium oxide nanoparticles into the CA nanofibers were incorporated to remove metal ions and dyes from water [26]. CA/TiO_2 composite nanofibrous adsorbent was synthesized for the removal of heavy metal ions [37]. The potential of CA/chitosan coated by ferrite nanoparticles for the adsorption of phenol and metal ions has been investigated [38]. Electrospun CA/hydroxyapatite nanocomposite nanofibers were synthesized for the adsorption of Fe(III) and Pb(II) from water [39]. Graphene oxide (GO), due to its large scale production, low cost, high mechanical properties, and hydrophilic nature, is often blended with the polymeric solution to obtain the composite nanofibers with improved mechanical strength and high removal efficiency [40–43]. The aim of this study is to incorporate the GO into the CA nanofibers for increasing the mechanical strength and adsorption capability of nanofibers toward Cr(VI) ions sorption.

The present work studies the capability of CA/GO composite nanofibers for the adsorption of Cr(VI) ions in a batch system under different adsorption variables such as contact time, adsorbent dosage, pH, Cr(VI) concentration, and temperature. The kinetic and equilibrium data of Cr(VI) adsorption by the composite nanofibers were analyzed by the pseudo-first-order and pseudo-second-order kinetic and Redlich-Peterson, Langmuir, Freundlich, isotherm models, respectively. The thermodynamic parameters were also investigated based on the impact of temperature on the Cr(VI) ions sorption using the CA/GO composite nanofibers.

2 Experimental

2.1 Materials and methods

Cellulose acetate (Mw:30 kDa, CA), and trifluoroacetic acid (TFA) supplied from Sigma-Aldrich (Germany) were used for the preparation of CA solutions. Cr(VI) ions solution was prepared by dissolving a predetermined amount of potassium dichromate (Sigma-Aldrich, Germany) in distilled water. The morphology and mean fiber diameter were determined by using a scanning electron microscope (JSM-6380, JEOL, Germany, SEM) and an image analyzer, respectively. The gold coating was implemented on nanofibrous samples using a sputter coater (Polaron, SC7620). The as-prepared nanocomposites were dispersed in water and cast onto a copper grid to study the size and morphology of the synthesized materials by TEM (Transmission Electron Microscope) using a Philips–CM300–150 kV microscope.

2.2 Preparation of CA/GO composite nanofibers

The modified Brodie method was used to synthesize graphite oxide nanosheets from graphite powder, potassium permanganate, sulfuric acid and orthophosphoric acid as described previously [44]. CA solution (10 wt.%) was prepared by dissolving 1 g CA in 10 mL TFA under stirring for 4 h. Various GO content (0, 0.5, 1, 1.5, and 2 wt.%) was added to the CA solution and sonicated for 30 min to prepare CA/GO solutions. The prepared solutions were transferred into a 5 mL plastic syringes attached to the syringe pump. The electrospinning condition for fabrication of CA and CA/GO nanofibers was an applied voltage of 20 kV, the feeding rate of 0.3 mLh^{-1}, the distance of 12 cm, the temperature of 25%, and the humidity of 40%.

2.3 Adsorption process in a batch system

Adsorption experiments were implemented by immersing 20 mg nanofibers (CA and CA/GO composite nanofibers) into the 250 mL flasks containing 100 mL of 50 mgL^{-1} Cr(VI) at 200 rpm and 25 °C. The effect of GO content (0–3 wt.%), pH (2–8), contact time (5–60 min), initial concentration of Cr(VI) (10–1000 mgL^{-1}), and temperature (25–45 °C) on the Cr(VI) sorption using nanofibers was investigated. The adsorption capacity (q mgg^{-1}) was evaluated based on the initial (C_0, mgL^{-1}) and equilibrium (C_e, mgL^{-1}) concentrations of adsorbate, solution volume (V, L) and nanofibrous adsorbent weight (g) as follows:

$$q_e = \frac{(C_0 - C_e)V}{M} \tag{1}$$

The known pseudo-first-order (Eq. 2), pseudo-second-order (Eq. 3) kinetic models and Freundlich (Eq. 4), Langmuir (Eq. 5), and Redlich-Peterson (Eq. 6) isotherm models were utilized for describing the kinetic and equilibrium data of Cr(VI) ions sorption using nanofibers [45]. The adsorption nature of Cr(VI) ions by the composite nanofibers was further investigated by evaluating the thermodynamic parameters such as Gibbs free energy change (ΔG°), enthalpy change (ΔH°), and entropy change (ΔS°). The reusability of nanofibers for Cr(VI) sorption was implemented for five cycles by their immersion in 1 M HCl for 2 h. The final concentration of Cr(VI) ions is measured by an inductivity-coupled plasma atomic emission spectrophotometer (ICP-AES, Thermo Jarrel Ash, Model Trace Scan).

$$\text{Pseudo} - \text{first} - \text{order } q_t = q_e(1 - \exp(-k_1 t)) \tag{2}$$

$$\text{Pseudo} - \text{second} - \text{order } q_t = \frac{k_2 q_e^2 t}{1 + k_2 q_e t} \tag{3}$$

$$\text{Freundlich } q_e = k_F C_e^{1/n} \tag{4}$$

$$\text{Langmuir } q_e = q_m \frac{bC_e}{1 + bC_e} \tag{5}$$

$$\text{Redlich} - \text{Peterson } q_e = \frac{PC_e}{1 + \alpha C_e^{\beta}} \tag{6}$$

3 Results and discussion

3.1 Morphology of GO and CA/GO composite nanofibers

SEM images from GO and GO-loaded CA nanofibers with various concentrations (0–2.5 wt.%) are presented in Fig. 1. As shown in the figure, the sheet structure with nano-scale thickness was obtained for synthesized GO. For pure CA, the homogenous nanofibers with free of beads with an average diameter of 210 ± 70 nm were achieved. By loading 0.5 wt.%

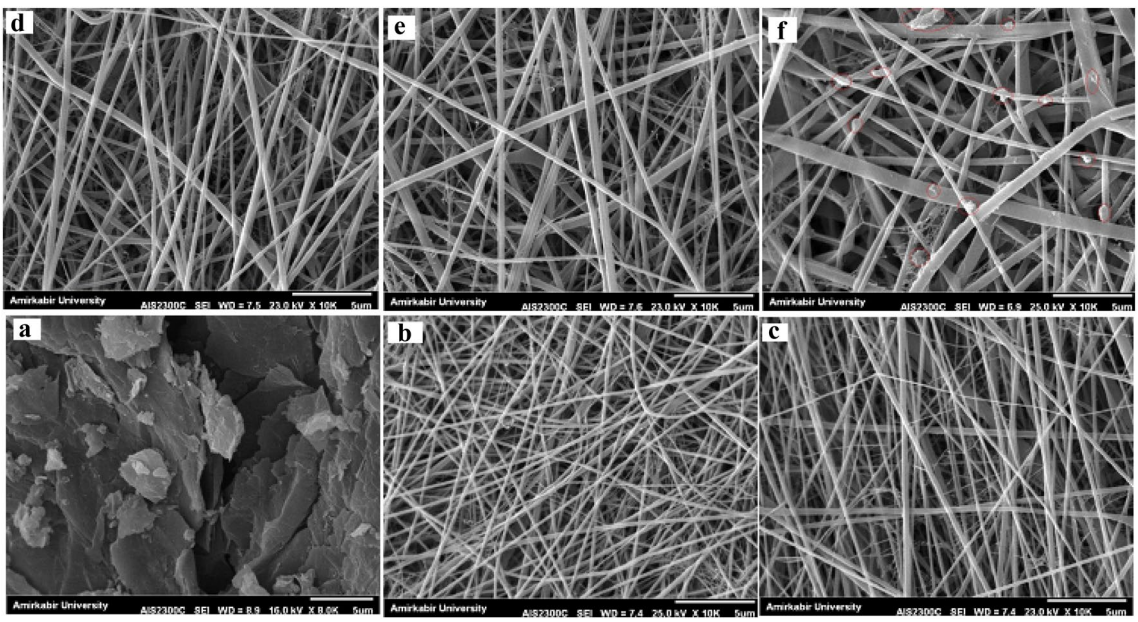

Fig. 1 SEM images from **a** GO, **b** CA, **c** CA/GO 0.5 wt.%, **d** CA/GO 1 wt.%, **e** CA/GO 2 wt.%, and **f** CA/GO 2.5 wt.% composite nanofibers

GO into the nanofibers, the fiber diameter was gradually increased due to its physical loading and increase in the solution viscosity. By increasing GO concentration up to 2 wt.%, the fiber thickness was increased and GO nanosheets were successfully incorporated into the nanofibers without aggregation in the nanofibers surface. By incorporating 2.5 wt.% GO, the fiber diameter was significantly increased and some GO have been aggregated on the surface of the nanofibers. The uniform dispersion of GO into the CA solution resulted in production of uniform nanofibers for CA/GO solutions containing 0.5, 1, and 2 wt.% with an average diameter of 260 ± 110, 320 ± 130, and 430 ± 140 nm, respectively. Whereas, the beaded-fibers with an average diameter of 530 ± 150 nm were obtained for CA/GO 2.5 wt.% composite nanofibers.

TEM images of the nanocomposites nanofibers are presented in Fig. 2. The images shown in the figure demonstrate the wire morphology of the nanocomposites. However, GO nanosheets exhibited a bulk structure (Fig. 2a). Figure 2b–f shows that compositing CA with GO increases the thickness size of the composite. According to the images, it is found that the thickness size of the structures is increased by increasing the GO weight content ratio in the nanocomposite mixture. According to the TEM images and the scale bar sizes, the thickness size of the rod-like structure samples is 50, 70, 120, 200, 300 nm, respectively, for CA, CA/GO 0.5 wt.%, CA/GO 1 wt.%, CA/GO 2 wt.%, and CA/GO 2.5 wt.% composite nanofibers.

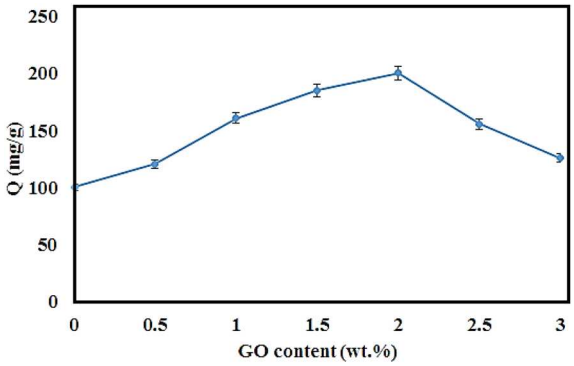

Fig. 3 Effect of GO content on the adsorption capacity of CA/GO composite nanofibers to Cr(VI) ions

3.2 Effect of GO concentration on Cr(VI) ions adsorption

The effect of GO content in the CA/GO nanofibers on the Cr(VI) adsorption capacity under 0.2 g/L adsorbent dosage, pH:2, Cr(VI) concentration of 50 mg/L, 25 °C, and GO content ranging from 0 to3 wt.% is presented in Fig. 3. As shown, by increasing GO concentration up to 2 wt.%, the adsorption capacity of Cr(VI) ions by the composite nanofibers was increased and further increase in GO content resulted in decreasing the adsorption capacity due to aggregation of GO on the nanofibers matrix and decreasing the available active sites for Cr(VI) ions sorption as confirmed by SEM images. By loading GO into the nanofibers up to 2 wt.%, the increase in the adsorption capacity of Cr(VI) ions by the composite nanofibers could be attributed to the high porosity, large specific area and higher available active

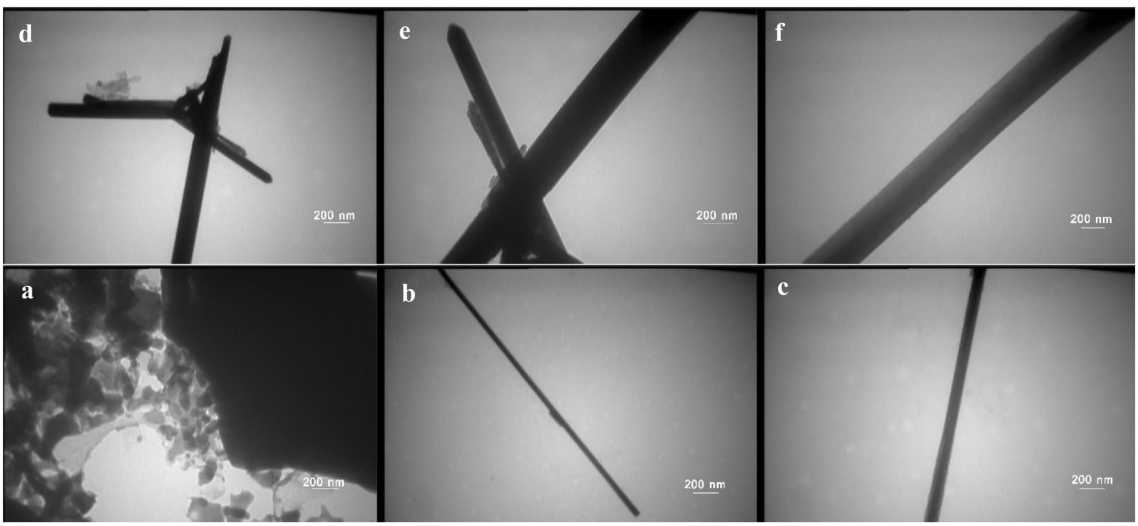

Fig. 2 TEM images of **a** GO, **b** CA, **c** CA/GO 0.5 wt.%, **d** CA/GO 1 wt.%, **e** CA/GO 2 wt.%, and **f** CA/GO 2.5 wt.% composite nanofibers

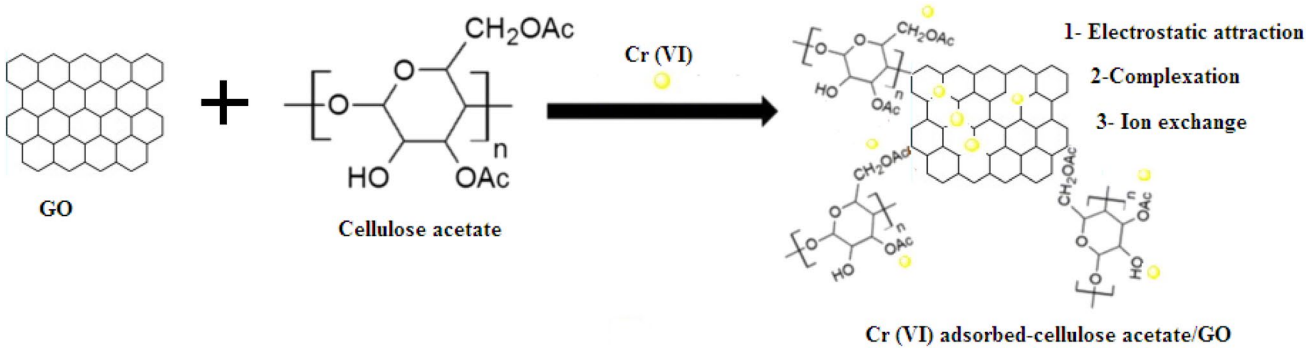

Scheme 1 Adsorption mechanisms of Cr(VI) ions using CA/GO composite nanofibers

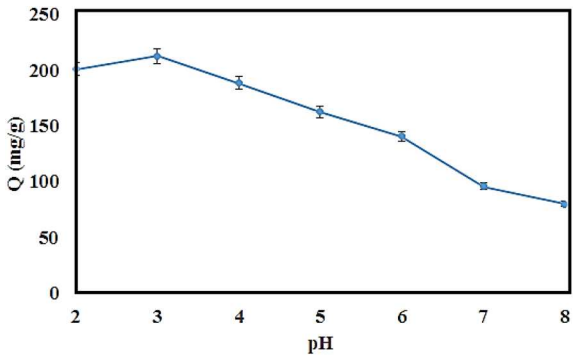

Fig. 4 Effect of pH on the adsorption capacity of CA/GO composite nanofibers to Cr(VI) ions

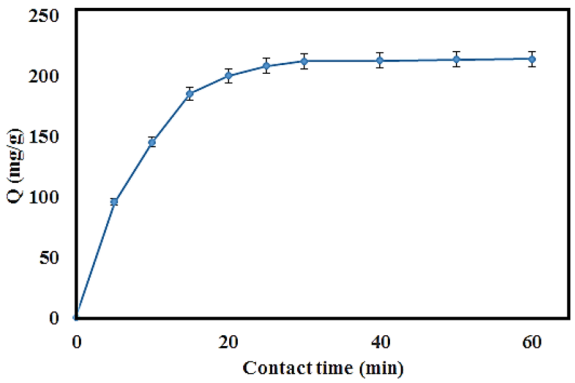

Fig. 5 Effect of contact time on the adsorption capacity of CA/GO composite nanofibers to Cr(VI) ions

sites of GO for Cr(VI) ions sorption. Moreover, the high amounts of hydroxyl groups of GO and the redox reaction of –OH groups with Cr(VI) ions led to the removal of Cr(VI) ions from water by loading GO and enhancement of GO content up to 2 wt.% [46]. Furthermore, hydroxyl groups of GO could be oxidized into the carboxylic acid by reducing Cr (VI) ions to Cr (III) ions. After that, Cr (III) ions could be easily adsorbed on the nanofibers surface. Moreover, the carboxylic groups of CA could bond with Cr (VI) ions, via the surface complexation mechanisms. Therefore, the main mechanisms to remove Cr(VI) ions, are absorbance through the nanofibers porosity, ionic exchange, surface complexation and reduction. The CA/GO 2 wt.% composite nanofibrous adsorbent is selected for further experiments. The schematic of Cr(VI) ions sorption mechanism using CA/GO composite nanofibers is illustrated in Scheme 1.

3.3 Effect of pH on the Cr(VI) ions sorption

The effect of pH on the Cr(VI) ions sorption using CA/GO 2 wt.% composite nanofibers under 0.2 g/L adsorbent dosage, Cr(VI) concentration of 50 mg/L, 25 °C, and different pH values ranging from 2 to 8 wt.% is presented in Fig. 4. As shown in the image, increasing pH value resulted in decreasing chromium ions adsorption capacity of composite nanofibers and the maximum adsorption capacity was found at pH = 3. The positive charge of CA and GO led to adsorb Cr(VI) ions ($HCrO_4^-$ and $Cr_2O_7^{2-}$) at pH 3. By increasing pH, the positive charge of the adsorbent was decreased, which resulted in decreasing the adsorption capacity. The significant decrease in Cr(VI) adsorption after pH = 7 could be attributed to the competition between chromium ions and hydroxyl groups, which blocked the large numbers of nanofibrous adsorbent active sites and significantly reduced its adsorption capacity. The obtained results indicated that the electrostatic interaction plays a significant role in the adsorption of Cr(V) ions by the composite nanofibers. Therefore, pH = 3 is selected for further experiments.

3.4 Effect of contact time on the Cr(VI) ions sorption and kinetic models

The impact of contact time on Cr(VI) ions sorption using CA/GO 2 wt.% composite nanofibers under 0.2 g/L adsorbent dosage, pH = 3, Cr(VI) concentration of 50 mg/L, 25 °C and contact time in the range of 5–60 min is presented in Fig. 5. It is found that the fast adsorption of

Table 1 Kinetic parameters of Cr(VI) ions sorption using synthesized nanofibers

Experimental	Pseudo-first-order				Pseudo-second-order			
$q_{t\ (mg\ g^{-1})}$	$q_{e\ (mg\ g^{-1})}$	$k_{1\ (min^{-1})}$	R^2	RMSE	$q_{e\ (mg\ g^{-1})}$	$k_{2\ (g.mg^{-1}.min^{-1})}$	R^2	RMSE
212.4	185.23	0.05428	0.965	5.241	224.5	0.00781	0.990	0.491

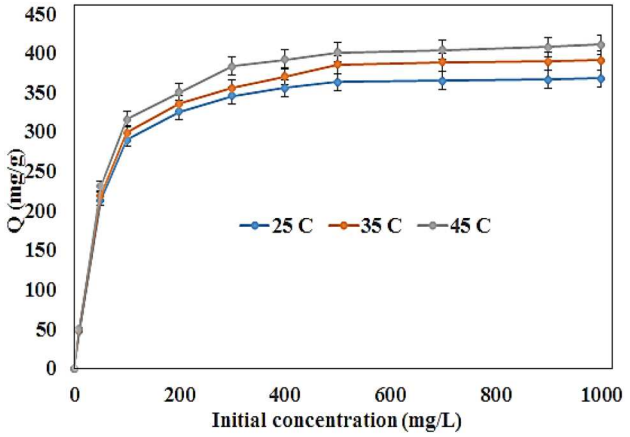

Fig. 6 Effect of initial concentration on the adsorption capacity of CA/GO composite nanofibers to Cr(VI) ions at different temperatures

Cr(VI) ions using CA/GO composite nanofibers occurred for 15 min and reached to equilibrium after only 30 min. The fast adsorption during 15 min could be attributed to the high surface area, high porosity and high amounts of functional groups for Cr(VI) ions sorption. The lower adsorption capacities of Cr(VI) ions by the adsorbent were due to the diffusion of Cr(VI) ions to the inner pores of nanofibers, and interaction of some functional groups of GO doped-CA nanofibers. Therefore, 30 min is selected as an equilibrium time for Cr(VI) ions sorption. The experimental Cr(VI) sorption data were fitted by pseudo-first-order, and pseudo-second-order kinetic models which results are presented in Table 1. The data revealed that the pseudo-second order kinetic model described the kinetic data of Cr(VI) ions sorption using the synthesized composite nanofibrous adsorbent. This behavior indicated that the chemisorption is a predominant mechanism for the Cr(VI) ions sorption by the CA/GO nanofibers.

3.5 Effect of initial concentration on the Cr(VI) ions sorption and isotherm models

The impact of initial concentration on the Cr(VI) ions sorption using CA and CA/GO 2 wt.% composite nanofibers under 0.2 g/L adsorbent dosage, pH = 3, contact time 30 min, 25 °C, and different initial concentrations ranging from 10 to 1000 mg/L is presented in Fig. 6. Figure 6 shows that increasing the Cr(VI) concentration increases the adsorption capacity of nanofibers toward Cr(VI) ions sorption up to an initial concentration of 500 mg/L Cr(VI) due to increasing the driving force. After that, the adsorption capacity did not change by further enhancement of Cr(VI) ions concentration due to the saturation of active sites of nanofibrous adsorbent.

The equilibrium data were analyzed by Freundlich, Langmuir, and Redlich-Peterson isotherm models. The results are presented in Table 2. The Redlich-Peterson isotherm model described well the equilibrium data of Cr(VI) ions sorption compared to the Langmuir and Freundlich isotherm models by comparing R^2 and RMSE values. The "n" value of Redlich-Peterson model was close to 1, which indicated that the monolayer sorption of Cr(VI) using synthesized nanofibers was predominant. The maximum experimental and monolayer sorption capacities of composite nanofibers for Cr(VI) sorption were about 410. 20 and 422.3 $mg.g^{-1}$, respectively, at 45 °C. The increasing the adsorption capacity by increasing temperature indicated that the higher temperature is favorable for the adsorption of more Cr(VI) ions from water. The units of T, K_F, q_{max}, K_L, P, and α are °C, $mg.g^{-1}$, $mg.g^{-1}$, $L.mg^{-1}$, $L.mg^{-1}$, and $L.mg^{-1}$, respectively.

3.6 Thermodynamic parameters for Cr(VI) ions sorption

Thermodynamic parameters are evaluated based on the thermodynamic equations and Van't Hoff plot of ln K_C versus 1/T as follows [47]:

Table 2 Isotherm parameters of Cr(VI) ions sorption using synthesized nanofibers at different temperatures

T	Freundlich isotherm					Langmuir isotherm				Redlich-Peterson isotherm				
	q_{exp}	K_F	n	R^2	RMSE	q_{max}	K_L	R^2	RMSE	P	α	n	R^2	RMSE
25	367.3	131.4	4.258	0.955	4.578	395.6	0.0457	0.982	2.774	22.11	0.524	0.915	0.993	0.482
35	390.2	142.5	4.444	0.962	4.014	408.8	0.0518	0.985	2.451	23.54	0.652	0.925	0.992	0.512
45	410.2	153.2	4.782	0.959	4.235	422.3	0.0548	0.988	2.154	25.31	0.845	0.948	0.994	0.459

Table 3 Thermodynamic parameters of Cr(VI) ions sorption using synthesized nanofibers

K_C			ΔH°	ΔS°	ΔG°		
25 °C	35 °C	45 °C			25 °C	35 °C	45 °C
4.12	13.42	25.31	100.899	0.3435	− 3.507	− 6.649	− 8.543

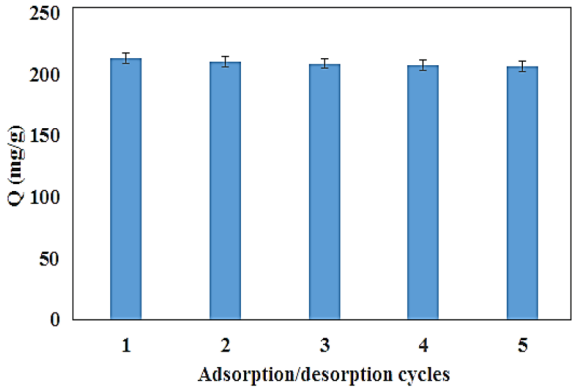

Fig. 7 Five adsorption–desorption cycles of Cr(VI) ions sorption by the CA/GO composite nanofibers

$$k_C = \lim_{C_{el} \to 0} \frac{C_{es}}{C_{el}} \tag{7}$$

$$\Delta G^0 = -RT \ln k_C \tag{8}$$

$$\ln k_C = \frac{\Delta S^0}{R} - \frac{\Delta H^0}{RT} \tag{9}$$

where R is the gas constant (8.314 J mol^{-1} K^{-1}), T is an absolute temperature (K) and k_C is the adsorption equilibrium constant. C_{es} and C_{el} are the values of solid-phase concentration and liquid phase concentration at equilibrium in mg L^{-1}. The results of Gibbs free energy change (ΔG^0), enthalpy change (ΔH^0), and entropy change (ΔS^0) of the adsorption process are listed in Table 3. The increasing the negative value of ΔG° (KJ/mol) by increase in temperature indicated the spontaneous nature of Cr(VI) ions sorption using nanofibers. The positive ΔH° (KJ/mol) values indicated the endothermic nature of the Cr(VI) ions sorption. The positive ΔS° value confirmed the enhancement of disorder in the solid-solution interface during the Cr(VI) ions sorption.

3.7 Reusability of nanofibers

The synthesized nanofibers regenerated successfully using 1 M HCl and used for five sorption/desorption cycles under 0.2 g/L adsorbent dosage, pH: 3, contact time 30 min, 25 °C and initial concentrations 50 mg/L, which results are presented in Fig. 7. The data indicated that the adsorption capacity did not significantly change after five cycles. The obtained results indicated the high capability of synthesized nanofiber for the adsorption of Cr(VI) ions from real wastewater in the future.

The maximum adsorption capacity of Cr(VI) ions using synthesized nanofibers was compared with other nanofibrous adsorbents in the literature, which results are presented in Table 4. As shown, the adsorption capacity of CA/GO composite nanofibers for Cr(VI) ions sorption was comparable and moderately higher than those of many corresponding nanofibrous adsorbents in the literature.

4 Conclusion

In this work, different GO concentrations (0–2.5 wt.%) were successfully loaded into the CA nanofibers to produce CA/GO composite nanofibers for the adsorption of Cr(VI) ions from aquatic systems. The mean fiber diameter of CA/GO nanofibers containing 0, 0.5, 1, 2, and 2.5 wt.% GO was about 210 ± 70 nm, 260 ± 110, 320 ± 130, 430 ± 140 nm,

Table 4 Comparison of adsorption capacity of Cr(VI) sorption using CA/GO nanofibers with other nanofibers in the literature [24, 25, 38, 48–52]

Adsorbent	Adsorbate	q_{max} (mgg^{-1})	Ref.
Chitosan/graphene oxide fibers	Cr(VI)	310.4	[24]
Chitosan-g-PNVCL/ZIF-8 nanofibers	Cr(VI)	495.6	[25]
CA/chitosan/Ferrite nanofibers	Cr(VI)	193.2	[38]
Chitosan/MWCNTs/Fe_3O_4 nanofiber	Cr(VI)	360.1	[48]
Polypyrrole-polyaniline	Cr(VI)	227.0	[49]
Polyacrylonitrile/NH_2 nanofibers	Cr(VI)	156.0	[50]
Stacked chitosan nanofibers	Cr(VI)	131.58	[51]
Sodium alginate-polyaniline nanofibers	Cr(VI)	73.34	[52]
CA/GO nanofibers	Cr(VI)	422.3	This study

and 530 ± 150 nm, respectively. The maximum experimental and monolayer adsorption capacities of CA/GO composite nanofibers for Cr(VI) sorption were about 410.20 and 422.3 $mg.g^{-1}$, respectively, under 2 wt.% GO, 0.2 g/L adsorbent dosage, pH: 3, contact time 30 min, and 45 °C. The spontaneous and endothermic nature of Cr(VI) sorption using the CA/GO nanofibrous adsorbent were obtained by evaluating thermodynamic parameters. Nanofibers were successfully regenerated for five adsorption–desorption cycles without significant change in the adsorption capacity of composite nanofibers for Cr(VI) ions sorption.

Declarations

Conflict of interest The authors declare that they have no competing interests or personal relationships that could have appeared to influence the work reported in this paper.

References

1. O.P. Temilade, O.J. Olubukola, W.A. Akinkunmi, H.O. Rukayat, Int. J. Biotechnol. **9**, 14–23 (2020)
2. P. Miretzky, A.F. Cirelli, J. Hazard. Mater. **180**, 1–9 (2010)
3. T. Dodderi, M. Puthiry, S. Thomas, Biol. Med. **11**, 169 (2020)
4. S.S. Shetty, M. Sharma, S.P. Kabekkodu, N.A. Kumar, K. Satyamoorthy, R. Radhakrishnan, J. Carcinogenesis **20**, 9 (2021)
5. S.R. Yadav, B. Goyal, R. Kumar, S. Gupta, A. Gupta, A.A. Mirza, G. Sharma, S. Rao, R. Pasricha, M. Gupta, J. Carcinogenesis **19**, 11 (2020)
6. H.N. Tran, D.T. Nguyen, G.T. Le, F. Tomul, E.C. Lima, S.H. Woo, A.K. Sarmah, H.Q. Nguyen, P.T. Nguyen, D.D. Nguyen, T.V. Nguyen, J. Hazard. Mater. **373**, 258–270 (2019)
7. M.A. Islam, M.J. Angove, DW Monitoring Manag. **12**, 100267 (2019)
8. M. Gheju, I. Balcu, J. Hazard. Mater. **196**, 131–138 (2011)
9. B. Daswani, Y. Khan, J. Carcinogenesis **20**, 9 (2021)
10. R.A. Siddeek, A. Gupta, S. Gupta, B. Goyal, A.K. Gupta, S. Agrawal, R. Roshan, U. Kumar, N. Kumar, M. Gupta, S. Kishore, J. Carcinogenesis **19**, 5 (2020)
11. K.D. Datkhile, S.R. Patil, M.N. Patil, P.P. Durgawale, N.J. Jagdale, V.N. Deshmukh, Studies on phytoconstituents. J. Nat. Sci. Biol. Med. **11**, 198–205 (2020)
12. K.K. Danaboina, P. Neerati, J. Nat. Sci. Biol. Med. **11**, 105–110 (2020)
13. M.N. Shalaby, Int. J. Pharmaceutical Res. Allied Sci. **7**(1), 126–132 (2018)
14. M.N. Shalaby, M.M. Sakoury, M.A. Kholif, N.I. Alsayed, J. Adv. Pharm. Educ. Res. **10**, 141 (2020)
15. M.M.A. Sakoury, M.N. Shalaby, A.M. Elmaghraby, I.M. Omar, M.M.A. Tahoun, Med. Sci. **24**, 143–164 (2020)
16 M.N. Shalaby, M. Saad, S. Akar, M. Abdelreda, A. Reda, A. Shalgham, J. Human Kinet. **35**, 69–79 (2012)
17. M.N. Shalaby, M.M.A. Sakoury, S.M. Harthi, F.M. Alshalawi, M.M. Alhajji, Z.H. Alshaikh, A.H. Aljaber, SRP **11**, 851–854 (2020)
18. D.O. Bokov, D.I. Karabeshkin, I.A. Samylina, O.G. Potanina, I.I. Krasnyuk, A.D. Malinkin, E.V. Sergunova, TYu. Kovaleva, N.V. Bobkova, A.M. Antsyshkina, A.A. Bondar, A.A. Evgrafov, E.K. Galiakhmetova, D.V. Moiseev, V.V. Bessonov, Pharmacogn. J. **12**, 415–421 (2020)
19. S. Wu, Y. Ge, Y. Wang, X. Chen, F. Li, H. Xuan, X. Li, Environ. Technol. **39**, 1937–1948 (2018)
20. M. Irani, L.R. Rad, H. Pourahmad, I. Haririan, Microporous Mesoporous Mater. **206**, 1–7 (2015)
21. M. Pishnamazi, S. Koushkbaghi, S.S. Hosseini, M. Darabi, A. Yousefi, M. Irani, J. Mol. Liq. **317**, 113934 (2020)
22. T. Xu, Y. Zhou, X. Lei, B. Hu, H. Chen, G. Yu, J. Environ. Manag. **249**, 109322 (2019)
23. L.R. Rad, M. Anbia, J. Environ. Chem. Eng. **9**, 106088 (2021)
24. H.H. Najafabadi, M. Irani, L.R. Rad, A.H. Haratameh, I. Haririan, RSC Adv. **5**, 16532–16539 (2015)
25. E. Bahmani, S. Koushkbaghi, M. Darabi, A. ZabihiSahebi, A. Askari, M. Irani, Carbohydr. Polym. **224**, 115148 (2019)
26. A. ZabihiSahebi, S. Koushkbaghi, M. Pishnamazi, A. Askari, R. Khosravi, M. Irani, Int. J. Biol. Macromol. **140**, 1296–1304 (2019)
27. S. Koushkbaghi, A. Zakialamdari, M. Pishnamazi, H.F. Ramandi, M. Aliabadi, M. Irani, Chem. Eng. J. **337**, 169–82 (2018)
28. P. Wang, L. Wang, S. Dong, G. Zhang, X. Shi, C. Xiang, L. Li, New J. Chem. **42**, 17740–17749 (2018)
29. Q.H. Li, M. Dong, R. Li, Y.Q. Cui, G.X. Xie, X.X. Wang, Y.Z. Long, Carbohydr. Polym. **253**, 117200 (2021)
30. S. Zhang, Q. Shi, G. Korfiatis, C. Christodoulatos, H. Wang, X. Meng, Chem. Eng. J. **387**, 124179 (2020)
31. L. Li, Y. Li, C. Yang, Carbohyd. Polym. **20**, 299–307 (2016)
32. R. Araga, C.S. Sharma, J. Polym. Environ. **27**, 816–826 (2019)
33. D.N. Phan, H. Lee, B. Huang, Y. Mukai, I.S. Kim, Cellulose **26**, 1781–1793 (2019)
34. L. Zhang, T.J. Menkhaus, J. Membr. Sci. **319**, 176–184 (2008)
35. W. Zhou, J. He, S. Cui, W. Gao, Fibers and Polymers. **12**, 431–437 (2011)
36. N.A. Amin, M.A. Mokhter, N. Salamun, W.M. Wan Mahmood, Membranes **11**, 546 (2021)
37. K.A. Gebru, C. Das, J. Water Process. Eng. **16**, 1–3 (2017)
38. A. Karamipour, P.K. Parsi, P. Zahedi, S.M. Moosavian, Int. J. Biol. Macromol. **154**, 1132–1139 (2020)
39. A.A. Hamad, M.S. Hassouna, T.I. Shalaby, M.F. Elkady, M.A. AbdElkawi, H.A. Hamad, Int. J. Biol. Macromol. **151**, 1299–313 (2020)
40. F. Du, L. Sun, Z. Huang, Z. Chen, Z. Xu, G. Ruan, C. Zhao, Chemosphere **239**, 124764 (2020)
41. N.M. Aboamera, A. Mohamed, A. Salama, T.A. Osman, A. Khattab, Cellulose **25**, 4155–4166 (2018)
42. Z.Q. Feng, X. Yuan, T. Wang, Chem. Eng. J. **392**, 123730 (2020)
43. A.I. Abd-Elhamid, M.R. El-Aassar, G.F. El Fawal, H.M. Soliman, Environ. Nanotechnol. Monitoring Manag. **11**, 100207 (2019)
44. F. Naseri, M. Irani, M. Dehkhodarajabi, Archives Civil Mech. Eng. **16**, 695–701 (2016)
45. V. Sabourian, A. Ebrahimi, F. Naseri, M. Irani, A. Rahimi, RSC Adv. **6**, 40354–40365 (2016)
46. P.C. Bandara, J. Peña-Bahamonde, Sci. Rep. **10**, 1–8 (2020)
47. L.R. Rad, A. Momeni, B.F. Ghazani, M. Irani, M. Mahmoudi, B. Noghreh, Chem. Eng. J. **256**, 119–127 (2014)
48. S. Jamshidifard, S. Koushkbaghi, S. Hosseini, S. Rezaei, A. Karamipour, M. Irani, J. Hazard. Mater. **368**, 10–20 (2019)
49. M. Bhaumik, A. Maity, V.V. Srinivasu, M.S. Onyango, Chem. Eng. J. **181**, 323–333 (2012)
50. M. Avila, T. Burks, F. Akhtar, M. Göthelid, P.C. Lansåker, M.S. Toprak, A. Uheida, Chem. Eng. J. **245**, 201–209 (2014)
51. L. Li, Y. Li, L. Cao, C. Yang, Carbohyd. Polym. **125**, 206–213 (2015)
52. R. Karthik, S. Meenakshi, Int. J. Biol. Macromol. **72**, 711–717 (2015)

Authors and Affiliations

Indah Raya[1] · Gunawan Widjaja[2] · Zaid Hameed Mahmood[3] · Abed J. Kadhim[4] · Kabanov Oleg Vladimirovich[5,6] · Yasser Fakri Mustafa[7] · Mustafa M. Kadhim[8,9] · Trias Mahmudiono[10] · Ismail Husein[11] · Leila Kafi-Ahmadi[12]

✉ Indah Raya
R.Indah2021@gmail.com

[1] Departement of Chemistry, Faculty Mathematics and Natural Science, Hasanuddin University, Makassar, South Sulawesi 90245, Indonesia

[2] Universitas Krisnadwipayana, Jatiwaringin, Indonesia

[3] Department of Chemistry, College of Science, Diyala University, Baqubah, Iraq

[4] Al-Nisour University College, Baghdad, Iraq

[5] Russia College of Technical Engineering, National Research Ogarev Mordovia State University, 68, Bolshevitskaya str., Republic of Mordovia, Saransk, Russia 430005

[6] The Islamic University, Najaf, Iraq

[7] Department of Pharmaceutical Chemistry, College of Pharmacy, University of Mosul, Mosul, Iraq

[8] Dentistry Department, Kut University College, Kut, Wasit, Iraq

[9] College of Technical Engineering, The Islamic University, Najaf, Iraq

[10] Departemen of Nutrition, Faculty of Public Health, Universitas Airlangga, FKM Unair Jl. Mulyorejo Kampus C, Surabaya 60115, Indonesia

[11] Department of Mathematics, Universitas Islam Negeri Sumatera Utara, Medan, Indonesia

[12] Department of Inorganic Chemistry, Faculty of Chemistry, Urmia University, Urmia, Iran